IEEE Access
Multidisciplinary | Rapid Review | Open Access Journal

Received December 6, 2021, accepted December 30, 2021, date of publication January 5, 2022, date of current version January 13, 2022.

Digital Object Identifier 10.1109/ACCESS.2022.3140488

Investigation of an Autonomous Tracking System for Localization of Radio-Tagged Flying Insects

CHANYOUNG JU, (Student Member, IEEE), AND HYOUNG IL SON, (Senior Member, IEEE)
Department of Convergence Biosystems Engineering, Chonnam National University, Gwangju 61186, Republic of Korea
Interdisciplinary Program in IT-Bio Convergence System, Chonnam National University, Gwangju 61186, Republic of Korea

Corresponding author: Hyoung Il Son (hison@jnu.ac.kr)

This work was supported by the Cooperative Research Program for Agriculture Science and Technology Development, Rural Development Administration, Republic of Korea, under Project PJ0147612021.

ABSTRACT The tracking of flying insects is one of the main challenges in the field of ecosystem and biodiversity protection. In the case of invasive insects such as Asian hornets, extensive considerations must be made in estimating the habitat because of the limitations of available sensors and environmental uncertainty. In this study, we propose an approach for localizing and autonomously tracking radio-tagged flying insects and developing an unmanned aerial vehicle (UAV)-based robotic system. The extended Kalman filter is applied to the received signal strength emitted from a radio telemetry transmitter to estimate the insect's position while reducing the measurement error and noise. The proposed autonomous tracking strategy involves a method in which the UAV rotates around one point to measure the signal strength and control its position in relation to the direction of the strongest signal. We also designed a system architecture that includes a tracking sensor system and a UAV system for radio-tagged flying insects. The effectiveness of the proposed system for estimating and autonomously tracking the target position was evaluated via numerical dynamics simulation. Furthermore, feasibility tests with unmanned ground vehicle replacements for insects and UAVs were performed to validate the proposed approach. Finally, to verify the UAV system, field tests were conducted to track a fixed radio-tagged flying target on a vast flatland. This study is unique because we propose and validate a novel mobile robot-based tracking system to localize radio tags of flying insects.

INDEX TERMS Radio-tagged flying insects, unmanned aerial vehicles, radio telemetry localization, autonomous tracking, sensor systems.

I. INTRODUCTION

Tracking wildlife is crucial to protecting and managing ecology and biodiversity. The radius of action, main habitat, and number of endangered species can be effectively identified by monitoring the movements of animals and insects. Therefore, studies have employed sensor networks for localization and tracking to identify the activities of dynamic animals [1], [2]. Recently, mobile vehicles and robots have been introduced to address environmental diversity and uncertainty and improve maneuverability [3]. Among them, aerial robots are attracting attention for solving problems by actively localizing and tracking flying targets without restrictions, which is an improvement from the potential movement of ground robots [4]. This study aims to investigate the use of an aerial robot (i.e., unmanned aerial vehicle (UAV)) system to localize and autonomously track the radio tags of flying insects.

With regard to tracking dynamic animals and small insects using UAVs, studies investigating the behavior of targets (ranging from large to small size) have been conducted [5]–[7]. Various localization, mapping, path planning, and autonomous tracking algorithms based on aerial robots for tracking wildlife (e.g., birds [8], yellow-eyed penguins [9], iguanas [10], rhinoceroses [11], carp [12], and bears [13]) have been proposed. However, because evaluating the impact of exotic species on the ecosystem in response to climate change is becoming increasingly important, tracking the movements of flying insects is required and poses a significant challenge.

For example, the yellow-legged or Asian hornet, also known as *Vespa velutina*, has caused tremendous damage to the beekeeping industry and ecosystems from Asia to Europe [14]. It also threatens people in urban areas.

The associate editor coordinating the review of this manuscript and approving it for publication was Gerardo Di Martino.

Nevertheless, no robotic system for estimating their location or tracking their path autonomously has been reported. Recently, tracking methods through which humans can listen to the output of an audio signal have been used to track them [15]. Furthermore, in [16], a study was conducted to track the Asian hornet using a fixed large harmonic radar instead of a robotic system; however, we intend to explore an active tracking method with unlimited tracking range. Tracking robotic systems for flying insects, such as the Asian hornet, are effective for managing alien species, protected species, and natural ecosystems; they further present the advantage of preserving biodiversity.

In summary, we aim to develop a mobile aerial platform capable of tracking flying insects. Animal tracking systems mainly include a (I) visual-sensor-based system (e.g., stereo camera and thermal camera), (II) satellite-based global positioning system (GPS) or Argos system, (III) radio-signal-based harmonic radar systems, radio frequency identification (RFID) systems, or radio telemetry systems [17], [18]. In this study, we aimed to develop a UAV-based tracking method for flying insects, and we considered three variables to evaluate the aforementioned systems: (i) the weight of the sensor to be attached to the target (e.g., transmitter and tag), (ii) weight of the sensor system to be attached to the UAV (e.g., receiver and camera), and (iii)traceable distance.

First, (I) is not impacted by (i) because the visual sensor is only attached to the UAV to track the flying target. However, this is not a suitable approach owing to its limited performance in terms of (iii). Nevertheless, some researchers attempt to visually track targets by attaching feather-like tags to the flying insects. However, in a dynamic and complex environment (e.g., the forest), it is practically impossible to track fast and flying insects using a visual sensor. Second, (II) excels in terms of (ii) and (iii); however, this approach is also ineffective because the sensors that could be attached to flying insects would have to be extremely small, and sensors of this size do not yet exist [19]. In our previous study [18], we confirmed that Asian wasps could fly only when the sensor attached to them weighed less than approximately 0.3 g. However, GPS sensors that weigh tens to hundreds of grams are generally commercialized. Finally, because (III) excels when evaluated based on (i), (ii), and (iii), we developed a UAV system for tracking flying insects proposed in this study, considering these three variables.

However, RFID has a limited detection distance (typically within 1–5 m) and is deployed only in specific environments [20]. Therefore, it is not suitable for actively tracking flying insects in the field. Consequently, most researchers use harmonic radar [16] or radio telemetry [15] to track the behavior, movement, and evolution of wildlife [21], fish [22], or insects. Generally, a harmonic radar uses fixed radars to track targets; hence, it has a fixed detection area (less than 500 m radius) and uses passive tags (no battery in the tag) such that the availability of the tag power is not continuous [23]. Although a dynamic harmonic radar system with a large vehicle exists, it is difficult to develop an autonomous UAV system (the objective of this study) using this approach because the payload of a UAV is usually less than 5 kg. Most harmonic radar systems that track small insects are static/fixed and feature large radars [16]. Therefore, a harmonic radar is not suitable for developing an autonomous UAV system with superior maneuverability and scalability.

In the case of radio telemetry using an active transmitter, the weight of the receiver is within the payload requirements of the UAV; hence, it can be deployed in a UAV-based autonomous tracking system [24]. However, it can only be used to track heavy insects because of the weight of the transmitter [23]. Furthermore, the effectiveness of radio telemetry for tracking flying species is impeded by its short tracking range (typically 100–500 m) [23]. Specifically, as the weight of a sensor and target size decrease, so does its traceable distance. Consequently, the trade-off between weight and distance is a critical problem. Therefore, this study aims to develop a radio telemetry-based autonomous UAV system that can track small radio tags of flying insects, such as wasps [25] and beetles [26].

TABLE 1. Flight property of *Vespa velutina*.

Travel Distance	Duration	Velocity	Reference
528 m	45 min	0.1956 m/s	[15]
351 m	96 min	0.0609 m/s	
1331 m	133 min	0.1668 m/s	
49 m	53 min	0.0154 m/s	
195 m	63 min	0.0516 m/s	
343 m	119 min	0.0480 m/s	
45 m	71 min	0.0106 m/s	
238 m	121 min	0.0328 m/s	
500 m	234 min	0.0355 m/s	[27]
1000 m	481 min	0.0346 m/s	
2000 m	1005 min	0.0332 m/s	
3000 m	4806 min	0.0104 m/s	

TABLE 2. Nesting characteristics of *Vespa velutina*.

Number of nests	Average Altitude (± standard deviation)	Max Altitude	Reference
3	11 (±1.00) m	12 m	[28]
4	3.8 (±2.85) m	8 m	[29]
10	15.1 (±5.92) m	27.5 m	[30]
49013	13.7 (±8.20) m	–	[31]
31	11.8(±6.19) m	27.5 m	[32]

A. PROBLEM STATEMENTS

We define the problem of estimating the position of the flying target using only the radio signal strength. The fundamental dimensions required for estimating the position of an object in space are as follows.

1) Range: the horizontal distance of a target from UAV.
2) Bearing: the horizontal angle between the direction of a target and UAV.
3) Altitude: the vertical distance of a target from UAV.

Here, we redefine the problem of whether the UAV system needs to estimate the altitude of the Asian hornet for autonomous tracking. First, we analyze the biological properties of Asian hornets.

1) FLYING ALTITUDE

Ref. [33] installed traps at different heights to measure the flying height of wasps. In the five experimental conditions, the *Chalcid wasps* were caught most often at 37 m. In the case of pollinating wasps, the most frequent height was 45 m in 2003 [34], 30 m in 2005 [35], and 25 m in 2013 [36]. Although the flight altitude of the Asian hornet has not yet been reported, we expect it to fly at a height lower or similar to the aforementioned height. This is because Asian hornets prefer to build nests on trees, shrubs, and roofs close to the ground (the average height is 10—20 m) [32].

2) FLYING SPEED

Table 1 summarizes the results of previous studies on how long the Asian hornet flies and how far they travel from the released point after the radio sensors are attached. Similarly, in [37], where the flight capacity of *Vespa velutina* was studied, the mean flight speed was reported to be 1.56 ± 0.29 m/s. However, considering the view of flight duration and velocity, the average velocity of the Asian hornet is less than 0.2 m/s (i.e., very slow).

3) HABITATS

Asian hornet species prefer to live in low forests and mountains, avoiding high-altitude climates. Table 2 lists the altitudes and areas of the Asian hornet nests. The experimental results confirm that the average height of the habitat is approximately 10—15 m. Therefore, considering the flying altitude, speed, and habitats, we can conclude that the flight altitude of Asian hornets is not very high, and its moving radius is within a dozen meters.

From a technical point of view, we considered whether we should track the height of Asian hornets via radio telemetry systems in terms of tracking resolution. Therefore, we reviewed studies related to the estimation and tracking of flying targets, such as birds and insects, based on the radio telemetry system. In a previous study [6], the average position error was 51.47 m. Other cases present hundreds of meters of tracking errors. Moreover, even when using a radio telemetry system with better performance than a small-sized radio tag, the position tracking error is 38.0 m [38] and 22.7–30.1 m [5] on average.

In summary, the localization of Asian hornets is not three-dimensional but two-dimensional from a resolution perspective, as shown in Figure 1a, because the tracking error with a radio telemetry system is dozens of meters. In addition,

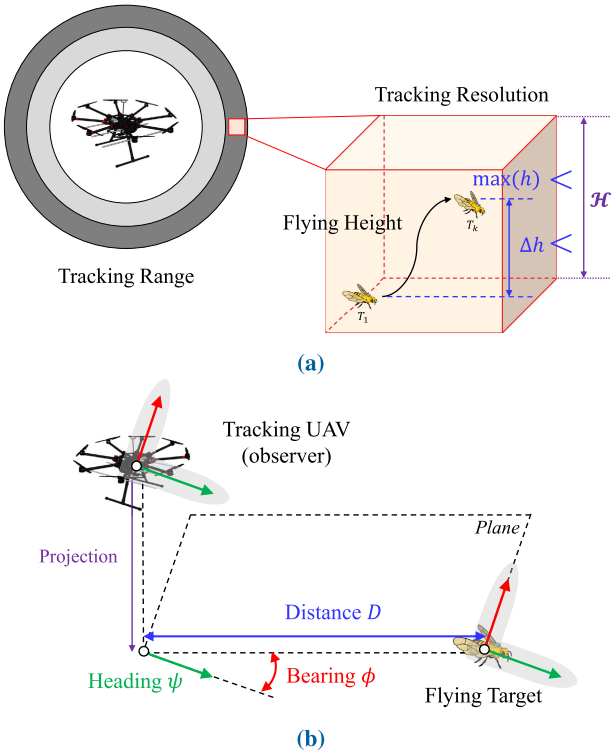

FIGURE 1. Problem definition of the tracking target. (a) Resolution. (b) Concept.

the main concept is an observer tracker, in which a UAV flies at higher altitudes than Asian hornets (Figure 1b). Consequently, in terms of the technical view regarding tracking resolution, the altitude frame is an extra degree of freedom (i.e., redundancy). Therefore, in this study, we estimated the relative distance and bearing of the flying target in a plane for tracking.

B. CONTRIBUTIONS

In this paper, we propose a mobile robot-based tracking strategy for localizing and autonomously tracking radio-tagged flying insects. In this system, the mobile robot autonomously tracks the estimated position of the target while receiving the signal strength emitted from a transmitter (radio telemetry). For localization, an extended Kalman filter was deployed to reduce the measurement error and noise. Autonomous tracking is a strategy for generating the path of a mobile robot by computing the strongest direction of the measured signal. We demonstrate the validity of the proposed system using dynamic simulations of tracking scenarios. Finally, we demonstrate the feasibility of the proposed system by implementing a real mobile robot and a small-sized radio tag with ideal size and weight to be attached to the Asian hornet. In summary, our main contributions are as follows:

1) We propose a systematic approach for localizing and autonomously tracking radio-tagged flying insects.
2) We design a mobile robot-based tracking system that provides solutions to overcome the limitations (e.g.,

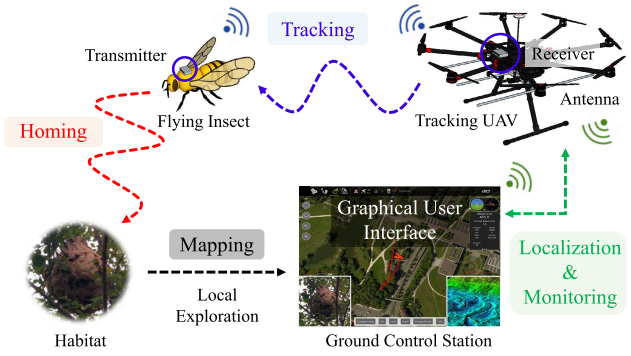

FIGURE 2. Concept of an aerial tracking system for radio-tagged flying insect.

small species and short tracking range) of existing radio telemetry systems.

3) We validate the feasibility of the proposed localization and autonomous tracking strategy for the radio-tagged target through numerical simulations, UGV-based feasibility tests, and UAV-based field tests.
4) We rigorously analyze and discuss the limitations of radio telemetry-based tracking systems and map out future research direction based on field tests.

C. STRUCTURE OF PAPER

The remainder of this paper is organized as follows. Sec. II introduces a mobile tracking system consisting of a tracking sensor system and a robot system for implementation, as well as the overall system architecture. Sec. III presents the localization and tracking strategy for radio-tagged flying insects. Sec. IV presents the experimental results that validate the proposed strategy and system; it also includes an in-depth discussion. Finally, Sec. V presents the concluding remarks and perspectives.

II. MOBILE TRACKING SYSTEM

In this study, a mobile robot-based tracking system is proposed to estimate and autonomously track the positions of radio-tagged flying insects. The principles of the proposed system are presented in Figure 2. The system is composed of a tracking sensor system and a UAV system. The radio telemetry-based tracking sensor system includes a transmitter, receiver, and Yagi antenna. The mobile robot system includes a flight controller, companion computer, and various sensors (e.g., barometer, gyroscope, magnetometer, and accelerometer).

A. TRACKING SENSOR SYSTEM

Table 3 shows representative small-sized transmitters for radio telemetry. When selecting a transmitter, one should consider that the lifespan of the battery is proportional to the weight of the sensor. The sensors described in Table 3 can be effectively attached to flying insects, such as Asian hornets and dragonflies because they can carry more than

TABLE 3. Radio transmitters for flying insects.

Model	Weight (g)	Lifespan (days)	Pulse Rate (ppm)	Company
NanoPin	0.13 g	7–29	30	Lotek
T15	0.15 g	13–26	15–30	ATS
PicoPip	0.20 g	4	30	Lotek
LB-2X	0.27 g	8–15	20–120	HOLOHIL
Micro model	0.27 g	15	30	PERDIX

TABLE 4. Specification of radio transmitter (LB-2X).

Specifications	Instructions
Frequency Range	148, 149, 150, 151, 164, 165, 172, 173, 218, 219, 220 MHz
Transmitter	Crystal-controlled two-stage design, pulsed by a multivibrator
Pulse Width	20 ms
Pulse Rate	20–120 pulses per minute (ppm), standard 40 ppm
Antenna	Single wire, 0.18 mm in diameter, 14–16 cm in length

TABLE 5. Specification of radio receiver (Australis 26k scanning receiver).

Specifications	Instructions
Frequency Range	4 MHz wide segments: select from 148.000–151.999 MHz, 149.000–152.999 MHz, 160.000–163.999 MHz, 170.000–173.999 MHz
Weight	1 kg with batteries
Sensitivity	10 dB S + S/N ratio at -135 dBm
Gain Control	Typically 100 dB
Selectivity	6 dB down at $\pm$ 0.8–1 kHz, 60 dB down at $\pm$ 5.5 kHz

approximately 0.30 g [15]. We chose LB-2X as the default transmitter in this study, considering the pulse rate and pulse length. The specifications of LB-2X are listed in Table 4.

Table 5 presents the specifications of the receiver (obtained from Titley Scientific Inc. in Australia) chosen to measure the radio signal from the transmitter. In general, the receiver has a dial-type gain regulator that adjusts the reception sensitivity and includes a variable resistor that controls the input voltage to the receiver controller. In other words, the receiver gain can be adjusted by outputting the desired voltage value through the analog output channel of the UAV controller without manually adjusting the dial. The corresponding voltage value is used to estimate the distance between the transmitter and receiver (i.e., flying insect and UAV).

The Yagi antenna possesses directivity, and its characteristics differ according to the antenna shape. The process of determining the directivity through experiments highly depends on the surrounding environment; furthermore, many

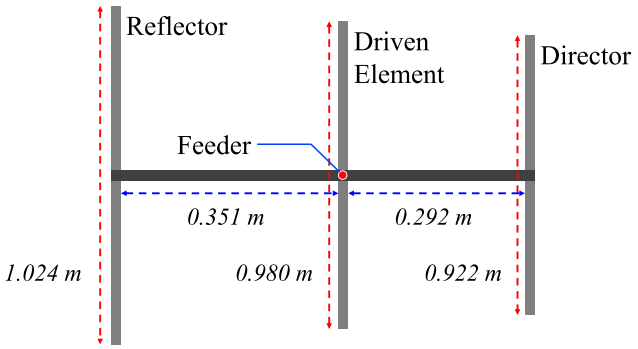

FIGURE 3. Modeling of a dedicated Yagi antenna.

TABLE 6. Specification of 3-element Yagi antenna (commercial).

Specifications	Instructions
Frequency Range	148.000–151.999 MHz
Elements	3
Bandwidth	± 2 MHz
Vertical Beamwidth	60°
Horizontal Beamwidth	100°
Gain	6 dB
Weight	400 g
Impedance	50 ohms

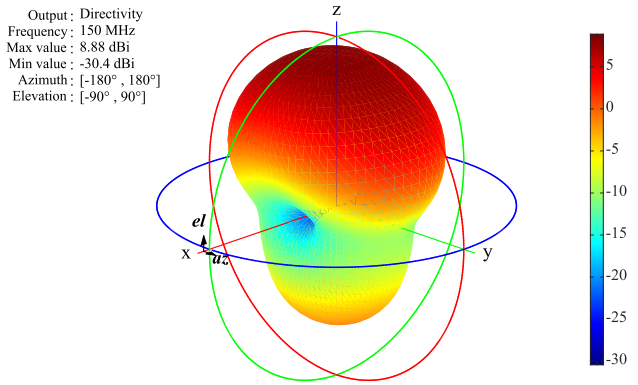

FIGURE 4. Radiation pattern of Yagi antenna.

experiments must be repeated to obtain the entire pattern. The ideal directivity of an antenna that is not under such an influence can be obtained in all directions through simulation. To analyze the directivity of the Yagi antenna—the specifications of which are listed in Table 6 and Figure 3—the antenna model was modeled in MATLAB (MathWorks Inc.) Antenna Toolbox. The antenna pattern depends on the radio frequency and the length of the reflector, driven element, and director, as shown in Figure 3.

Figure 4 shows the directivity at each position of the dedicated Yagi antenna. Note that the directivity is at its highest at 0°, when the antenna is placed horizontally on the ground (i.e., azimuth = 0°). Furthermore, the radiation pattern of the

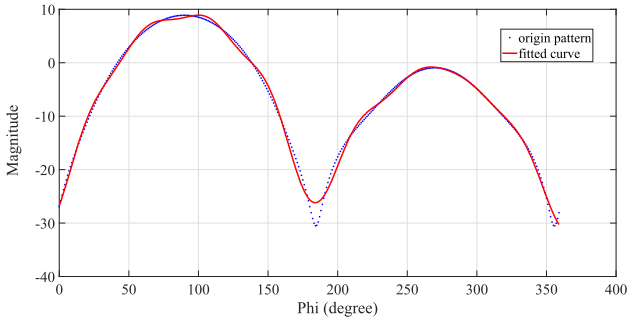

FIGURE 5. Curve fitting of directivity pattern (azimuth = 0°).

TABLE 7. Eighth-order Fourier series and estimated value for each parameter.

$f(x) = a_0 + \sum_{i=1}^{8} a_i cos(iwx) + b_i sin(iwx)$	
Parameters	Estimated value (with 95% confidence bounds)
a_0	−7.628 (−7.979, −7.278)
a_1	−1.668 (−2.201, −1.135)
b_1	6.351 (6.16, 6.543)
a_2	−13.54 (−13.71, −13.38)
b_2	3.851 (2.784, 4.919)
a_3	0.2556 (0.1202, 0.391)
b_3	1.269 (1.142, 1.1395)
a_4	−3.289 (−3.509, −3.068)
b_4	1.947 (1.429, 2.465)
a_5	0.2028 (0.072, 0.3337)
b_5	0.3186 (0.1867, 0.4506)
a_6	−1.23 (−1.566, −0.8936)
b_6	1.47 (1.165, 1.775)
a_7	0.529 (0.4021, 0.6558)
b_7	0.1259 (−0.09576, 0.3475)
a_8	−0.4146 (−0.6521, −0.1772)
b_8	0.8652 (0.711, 1.019)
w	0.01665 (0.01644, 0.01686)

Yagi antenna (azimuth = 0°) can be expressed in a rectangular coordinate system as per the blue dotted line in Figure 5. Furthermore, an eighth-order Fourier series was used for curve fitting, as presented in Table 7, and the result is depicted by the red solid line in Figure 5. The obtained mathematical model of the directivity of the antenna is applied to the UAV controller to determine the direction of the transmitter. For validation of the tracking sensor system, a preliminary study was conducted to analyze the signal strength, range, and tendency based on the selected radio system [18].

B. MOBILE ROBOT SYSTEM

An octocopter with a large payload was built to carry the radio telemetry receiver and Yagi antenna. Pixhawk 2 was used as a flight controller to control the UAV directly with various sensors, and Raspberry Pi 3 was used as the companion/onboard computer (computing module) and integrated the high-level

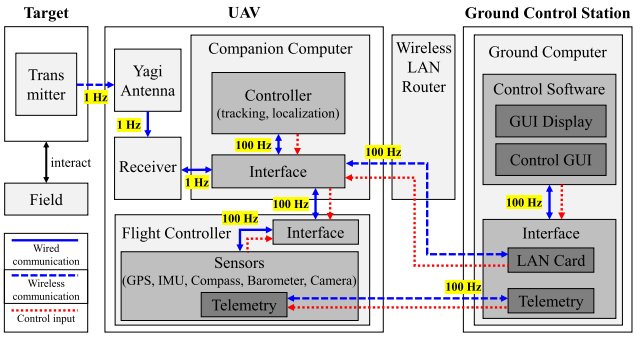

FIGURE 6. Tracking system architecture.

controller. The companion computer communicates with the radio receiver by converting RS232 to USB communication. Specifically, the voltage input for gain control can be directly provided to the receiver connected to the Yagi antenna using a coaxial cable. Data are transmitted from the signal of the transmitter attached to the flying insect in the order of antenna, receiver, and companion computer.

Figure 6 shows a diagram of the UAV-based tracking system architecture. The solid blue line represents wired communication, blue dotted line represents wireless communication, and red dotted line represents the control input signal. The UAV and estimated target positions are displayed in the software of the ground control station via a telemetry radio and LAN card. Each communication protocol and controller was implemented using a robot operating system (ROS) with a control rate of 100 Hz. The path through which the UAV should fly is also computed by the onboard computer, and the position and velocity of the UAV can be controlled through the ROS and MAVLink protocols. Low-level commands are sent from the high-level controller to the flight controller, and Pixhawk directly controls the motor.

III. TARGET LOCALIZATION AND TRACKING

A. EXTENDED KALMAN FILTER-BASED ESTIMATION

In this study, we focus on range-based measurements and received signal strength indicator (RSSI), which is used as a representative tracking approach for dynamic targets. The extended Kalman filter is deployed to improve the localization of the radio-tagged flying target while reducing the measurement noise.

1) EXTENDED KALMAN FILTERING

The extended Kalman filter is a recursive filter that estimates states based on measurements that contain noise or error [39]. It is mainly used for localization and tracking. Therefore, the extended Kalman filter estimates the state of the dynamic system, modeled as

$$x_k = f(x_{k-1}) + w_k \tag{1}$$

where x_k is the state vector at time k, f is the state transition function that is applied to the previous state x_{k-1}, and $w_k \sim \mathcal{N}(0, Q_k)$ is a random variable that represents the process noise, which is normally distributed with zero mean and covariance matrix, Q_k.

The observation (or measurement) term, z_k, of the true state, x_k, is defined as

$$z_k = h(x_k) + v_k \tag{2}$$

where h is the observation function that links the current state, x_k, to the observed measurement, z_k, at time t, and $v_k \sim \mathcal{N}(0, R_k)$ is the observation noise, which is assumed to be zero-mean Gaussian white noise with covariance matrix, R_k.

The extended Kalman filter involves a series of processes consisting of two states: time update (i.e., prediction) and measurement update (i.e., correct) [39].

The uncertain state of the RSSI is estimated and updated recursively using the extended Kalman filter.

2) MEASUREMENT MODEL

The update process of the extended Kalman filter requires a model of the measurement or system. In our approach, it is necessary to define a signal propagation model because the UAV tracks the signal strength emitted from the radio tags. Therefore, we deploy the log-distance path loss model—a signal propagation model that is suitable for representing RSSI measurements [40]. The log-distance path loss model that correlates the distance between the transmitter and receiver based on the RSSI is defined as

$$\mathbf{h}_\psi(\mathbf{x}, \mathbf{O}) = P_{d_0} - 10\, n \log \frac{D_\psi(\mathbf{x}, \mathbf{O})}{d_0}, \tag{3}$$

where $\mathbf{h}_\psi(\mathbf{x}, \mathbf{O})$ is the RSSI measurement function between the target's position, $\mathbf{x} \in \mathscr{R}^2$, and the observer's position, $\mathscr{O} \in \mathscr{R}^2$. The heading angle ψ; P_{d_0} is the RSSI at the reference distance, d_0; n is an environmental factor ranging from 2 to 4 (i.e., path loss exponent), and $D_\psi(\mathbf{x}, \mathbf{O})$ is the Euclidean distance between x and $\mathscr{O}$. In this equation, $D_\psi(\mathbf{x}, \mathbf{O})$ can be obtained by substituting $\mathbf{h}_\psi(\mathbf{x}, \mathbf{O})$ for P_{D_ψ} (RSSI) calculated at any $D_\psi(\mathbf{x}, \mathbf{O})$. The reference values of the parameters were determined in a previous study [18]. In addition, the f function of the extended Kalman filter is defined as

$$f(\mathbf{x}, \mathbf{O}) = \Delta \mathbf{h}_\psi(\mathbf{x}, \mathbf{O}). \tag{4}$$

In field environments, such as forests and nonurban areas, the RSSI is significantly affected by noise. Assuming that these noises are white, the total RSSI measurement $\mathbf{z}$ is defined as

$$\mathbf{z} = \mathbf{h}_\psi(\mathbf{x}, \mathbf{O}) + v, \tag{5}$$

where $v \sim \mathcal{N}(0, \sigma_R^2)$ is the white noise term, modeled as zero-mean Gaussian noise with covariance σ_R^2. Here, we assume that it is practical to characterize the received noise as white Gaussian, even if the RSSI noise in the field does not fully conform to the white noise model.

Algorithm 1 Tracking Strategy

input: orientation $\phi_i = \{\phi_1, \phi_2, \ldots, \phi_\alpha\}$, UAV current position $\mathcal{O}$, UAV current heading ψ, desired distance D_o, waiting time threshold T_d
UAV position input $\mathcal{O}_d \leftarrow \mathcal{O}$
UAV heading input $\psi_\mathbf{d} \leftarrow \psi$
$D_\psi(\mathbf{x}, \mathbf{O}) \leftarrow D_0 + C$
while $D_\psi(\mathbf{x}, \mathbf{O}) \leq D_o$ **do**
  $\alpha \leftarrow 0$
  for $i = 1$ to α **do**
    $\psi_\mathbf{d} \leftarrow \phi_i$
    Compute $\mathbf{h}_{\phi_i}(\mathbf{x}, \mathbf{O})$, $D_{\psi_i}(\mathbf{x}, \mathbf{O})$ by ((3))
    $\alpha \leftarrow max(\alpha, \mathbf{h}_{\phi_i}(\mathbf{x}, \mathbf{O}))$
  end for
  for $j = 1$ to k **do**
    if $\mathbf{h}_{\phi_j}(\mathbf{x}, \mathbf{O}) = \alpha$ **then**
      $D_\psi(\mathbf{x}, \mathbf{O}) \leftarrow D_{\phi_j}(\mathbf{x}, \mathbf{O})$
      $\psi_\mathbf{d} \leftarrow \phi_j$
      $\mathcal{O}_d \leftarrow \mathcal{O}_d + D_{\phi_j}(\mathbf{x}, \mathbf{O}) \frac{\boldsymbol{\psi}_\mathbf{d}}{||\boldsymbol{\psi}_\mathbf{d}||}$
    end if
  end for
  Time.sleep(T_d)
end while
output: $D_\psi(\mathbf{x}, \mathbf{O})$, $\psi_\mathbf{d}$

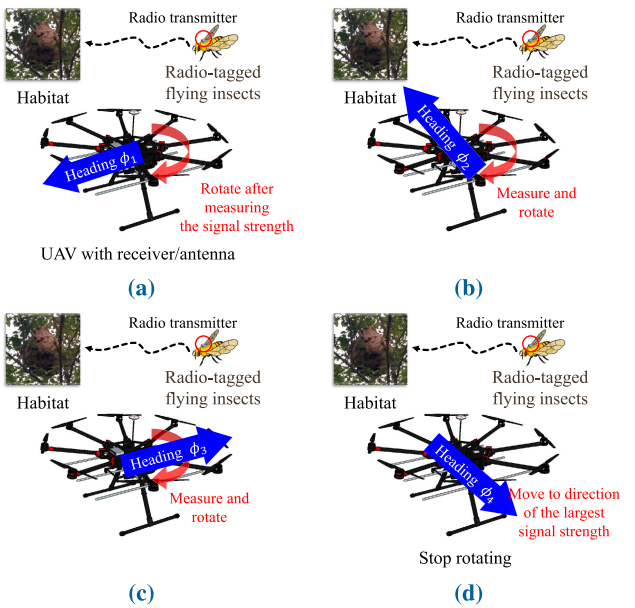

FIGURE 7. UAV-based autonomous tracking strategy. (a) Step 1 (b) Step 2 (c) Step 3 (d) Step 4.

B. AUTONOMOUS TRACKING STRATEGY

The UAV-based tracking algorithm is described in Algorithm 1. In Algorithm 1, the relative distances $D_\psi(\mathbf{x}, \mathbf{O})$ and direction $\psi_\mathbf{d}$ are predicted based on the RSSI and the designed measurement model discussed in the previous section. Furthermore, the controlled behavior of the UAV and the proposed tracking strategy for radio-tagged flying insects are detailed in Figure 7. Because the speed of the signal emitted from the transmitter is exceptionally low, if the UAV rotates 10° when measuring the signal in each direction, it requires 30 to 60 s to turn 360° even if the rotation time of the UAV is excluded. Because the position of the target (i.e., flying insect) varies with time, the rotation time must be minimized. In this study, the UAV aims to track the target when measuring the signal for only four orientations ϕ_α (i.e., 0, 90, 180, and 270°), $\alpha = 4$. This is achieved through the following steps.

1) The moving UAV stops and measures the RSSI at the current position (Figure 7a).
2) The UAV rotates in place at a certain angle (e.g., 90° in clockwise direction) to measure the signal strength. (Figure 7b and Figure 7c).
3) The direction in which the RSSI is the strongest is regarded as the direction in which the target is located, and the UAV advances in the corresponding direction (Figure 7d). Because the UAV can be translated into a space, it is possible to reduce the rotation time by reducing one step to return to its initial direction (that is, the direction shown in Figure 7a).
4) Although the localization approach is range-based, the UAV can move the distance in the estimated direction based on the tracking strategy because it is also interested in the RSSI measured in the radiation direction of the antenna (blue-colored arrows in Figure 7).
5) Even if the target stops at the habitat, the tracking process continues until the relative distance between the UAV and the target decreases by a certain distance (threshold D_o). Therefore, the tracking process is complete when the relative distance is sufficiently small. Finally, waiting duration T_d considers the rest time of flying insects carrying heavy tags.

As a result, the UAV tracker $\mathbf{O}$ can autonomously follow the target position $\mathbf{x}$ when estimating the direction, $\phi_\mathbf{d}$, and the relative distance $D_\psi(\mathbf{x}, \mathbf{O})$ based on Algorithm 1. This study considered only four orientations, ϕ_α; however, α could be increased for precise tracking.

IV. EXPERIMENTS AND DISCUSSIONS

A. DYNAMIC SIMULATIONS

To validate the tracking strategy, a software-in-the-loop simulation was performed using the robotic simulation software program Gazebo with the ROS, as shown in Figure 8. We assume that the average speed of the flying insect is 3 m/s, which is faster than that reported in previous studies [37], considering the Gaussian random function. Therefore, we estimated the position of the target based on the constant velocity model. We also assume that the insect moves from the starting position (i.e., the releasing location) to the target position (i.e., habitat) along the path. Moreover, the path of the flying insect was planned to be straightforward. The movement of a flying insect is depicted

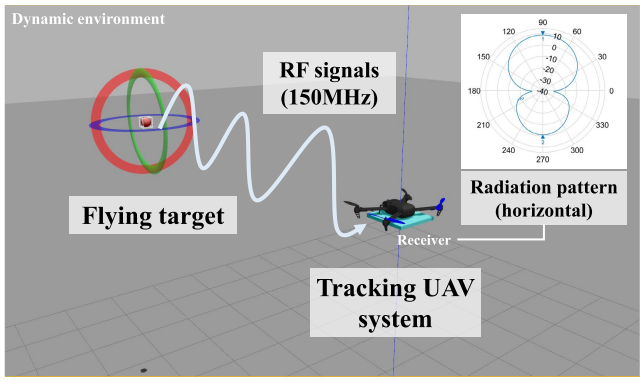

FIGURE 8. Simulation environments.

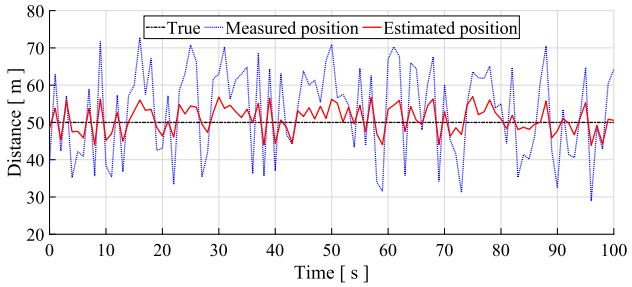

FIGURE 9. Localization result for static object.

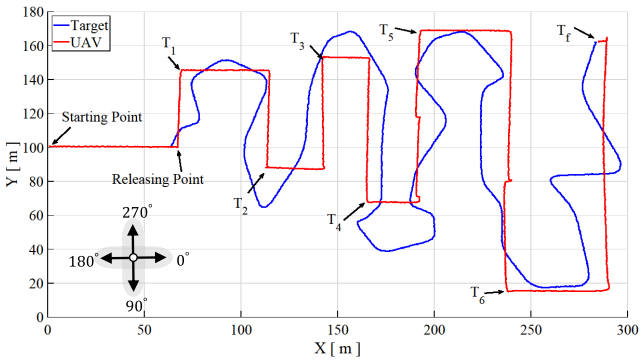

FIGURE 10. Simulation 1 results: path of target and UAV.

as the dynamic movement of a spherical point. An Iris+ model of 3DR Inc. was adopted as the tracking UAV; this model exhibits dynamic characteristics in this simulator. We assumed that the flying insect and UAV floated at the same height (5 m). The UAV has a maximum flight speed of 3 m/s. Therefore, the transmitter attached to the flying insect generates a signal of the same intensity at 1 Hz (frequency range of 150 MHz). The mathematical model of the receiver and antenna (calculated in Sec. II) was implemented using a dynamic simulator. This receiver can change the gain value by modifying the voltage input. However, in this experiment, the gain was constant. The RSSI calculated from the directivity model is transferred to the companion computer (system memory), and the UAV moves over a relative distance in the direction with the largest RSSI.

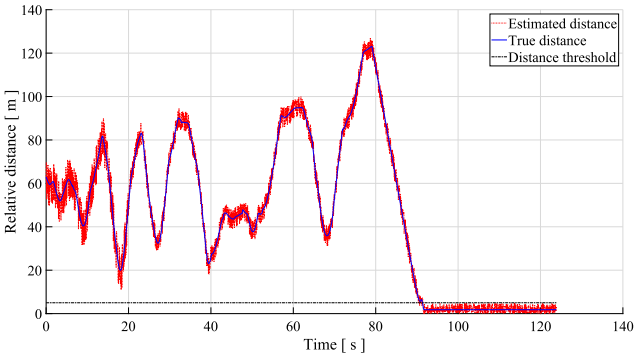

FIGURE 11. Simulation 1 results: relative distance of target from UAV.

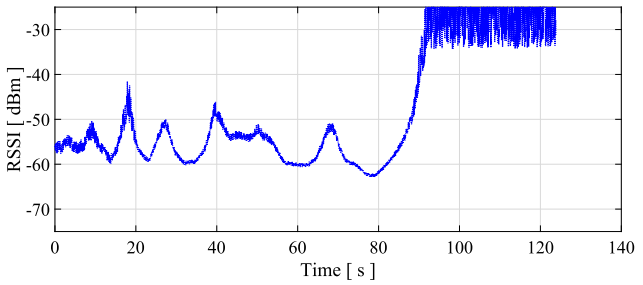

FIGURE 12. Simulation 1 results: measured RSSI.

B. SIMULATION RESULTS

Figure 9 shows the localization results for static objects in dynamic environments. In this experiment, the target position was set in a straight line 50 m away from the static UAV. Therefore, the black line represents the true value of the relative distance between the UAV and the target, the blue line represents the distance calculated by the sensor system, and the red line represents the distance estimated by the designed filter. The estimated value in this experiment shows the results of a 49.78 m average and 4.02 m standard deviation. This can be attributed to the uncertainty of the mathematical model in designing the system and the influence of various noise and measurement errors in a dynamic environment. Although both the target and the UAV are stationary, the experimental results indicate that the localization in the proposed system yields sufficiently reliable accuracy to facilitate improved tracking performance.

Figures. 10, 11, 12, and Table 8 show the results of the localization and tracking experiments for dynamic targets using the UAV-based system. In Figure 10, the path of the radio-tagged flying insects (blue line) and the tracking UAV (red line) are presented in X–Y coordinates. In the case of the dynamic target, the flight starts from the releasing point to the final point described in Figure 10, and the UAV autonomously tracks the radio signal emitted from the dynamic target. Figure 10 also clearly shows that the UAV tracks the radio-tagged target with utmost precision. Although the relative distance may increase without ever decreasing, the UAV can track the target while meeting the distance threshold. In the simulation results, we defined the time at which the UAVs reached the

TABLE 8. Experimental results of dynamics simulation.

Position	Orientation	RSSI	Distance	Relative distance
T_1	0°	−54.988	51.868	56.383 m
	90°	−56.328	60.520	
	180°	−58.614	78.7451	
	270°	−58.412	76.93	
T_2	0°	−56.195	59.601	61.880 m
	90°	−57.214	67.019	
	180°	−60.003	92.395	
	270°	−57.386	68.360	
T_3	0°	−58.056	73.839	70.477 m
	90°	−59.417	86.367	
	180°	−60.145	93.918	
	270°	−59.686	89.084	
T_4	0°	−44.797	28.533	27.513 m
	90°	−45.183	16.774	
	180°	−47.642	22.264	
	270°	−46.039	18.512	
T_5	0°	−53.705	44.745	48.274 m
	90°	−54.133	47.006	
	180°	−55.920	57.743	
	270°	−55.247	53.438	
T_6	0°	−59.415	86.353	84.715 m
	90°	−60.153	94.005	
	180°	−61.108	104.930	
	270°	−60.441	97.174	
T_f	0°	−30.415	3.064	1.794 m
	90°	−30.615	3.135	
	180°	−31.052	3.297	
	270°	−30.281	3.017	

final position as T_f, $\frac{1}{7}T_f$ as T_1, $\frac{2}{7}T_f$ as T_2, …, and $\frac{6}{7}T_f$ as T_6 to present measurements.

The variation in the distance between the dynamic target and UAV over time is depicted by the blue line in Figure 11. The distance between the UAV and the flight target decreases and increases during the tracking process. The distance between the two gradually decreases to approximately 80 s because the flying insect reaches the habitat and stops moving, and the UAV continues to move to that location. Here, we assume that the dynamic target remains in the habitat for a certain period of time. Before the target stops (i.e., before 80 s elapse), the relative distance of the UAV to the target decreases or increases because the UAV continues to repeat the localization and tracking process. Furthermore, the relative distance varies owing to the UAV angular velocity and slow flight compared to those of the radio-tagged target. After the UAV closes in on the flying insect, if the relative distance, $D_\psi(\mathbf{x}, \mathbf{O})$, is smaller than D_o, the desired distance set in Algorithm 1, it can be deduced that the UAV has stopped the tracking process, as shown in Figure 11 (after approximately 90 s). Figure 11 also shows the results of the localization (marked by the red line) performed on the

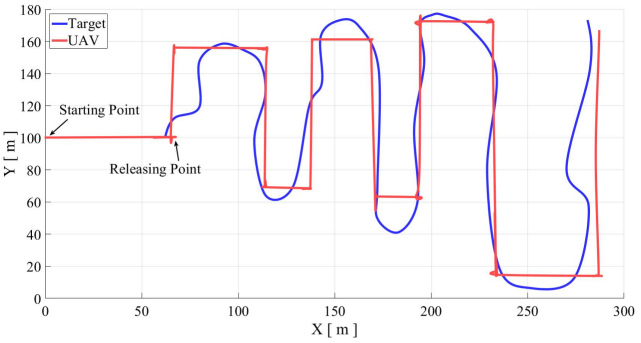

FIGURE 13. Simulation 2 results: path of target and UAV.

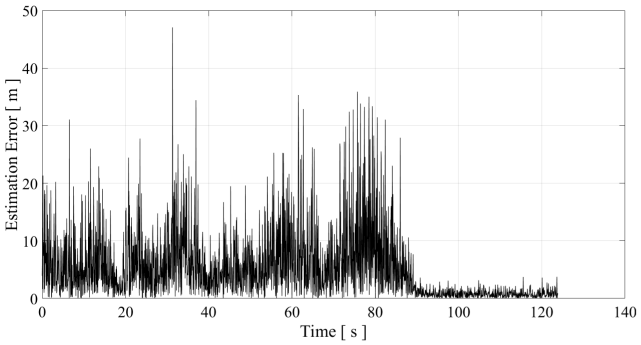

FIGURE 14. Simulation 2 results: estimation error.

dynamic target over time. This value indicates that $D_\psi(\mathbf{x}, \mathbf{O})$ is calculated using the extended Kalman filter-based localization algorithm. However, this value is the radius of a certain range, not distance, in range-based localization. In our tracking strategy, we set this radius to a scalar quantity in the ψ direction. Compared to the blue line, which shows the actual relative distance, the estimated distance shows the performance with an estimated error. In other words, in the case of the localization result (80 s), the actual relative distance is approximately 120 m. However, the estimated distance is approximately 130 m. This performance (i.e., localization of the radio-tagged flying insect) is inferior to the localization of static targets owing to the system or measurement noise. Nevertheless, the influence of the error can be disregarded when the distance between the UAV and the target is sufficiently small. Additionally, Figure 12 shows the calculated RSSI during dynamic experiments. Considering the estimated distances shown in Figure 11, the RSSI converges to a value of −25 dBm when the relative distance is small enough to close and follows the log scale with distance.

Table 8 lists values of the computed RSSI and estimated distance at a defined time. ψ denotes the heading angle of the UAV, $\mathbf{h}_\psi(\mathbf{x}, \mathbf{O})$ represents the RSSI measurement, $D_\psi(\mathbf{x}, \mathbf{O})$ represents the estimated relative distance, and the extra value indicates the actual relative distance. That is, the UAV estimates the direction in which the target is located through the $\mathbf{h}_\psi(\mathbf{x}, \mathbf{O})$ function. Once the direction is determined, the UAV flies to track the radio-tagged flying insect based

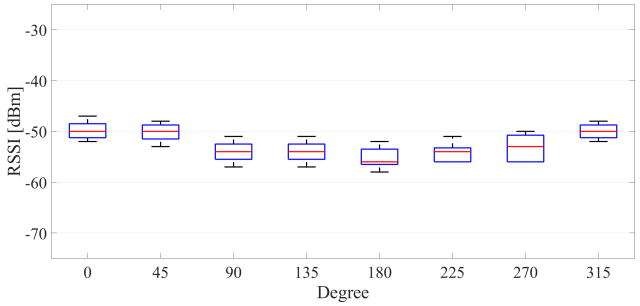

FIGURE 15. Experimental results of RSSI tendency.

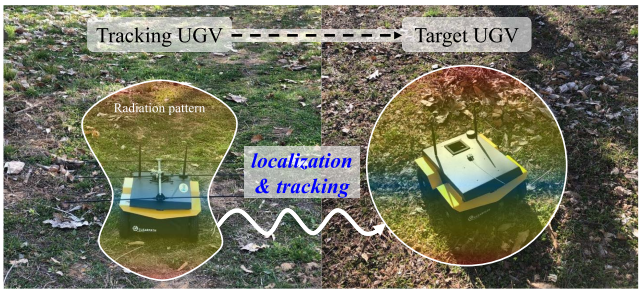

FIGURE 16. Experimental setup for tracking dynamic target.

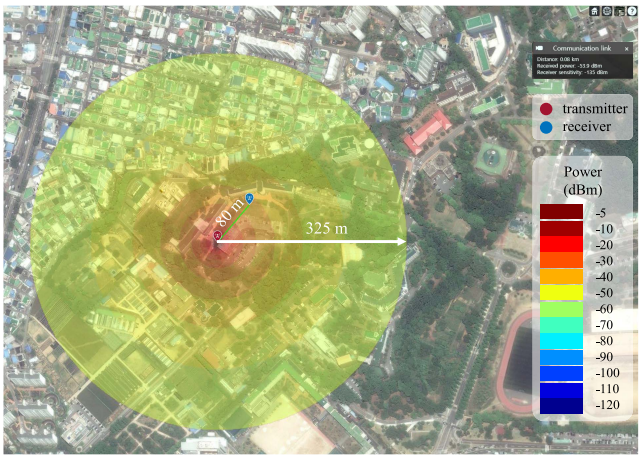

FIGURE 17. Ideal range of radio propagation for transmitter.

on $D_{\psi}(\mathbf{x}, \mathbf{O})$. In this process, the extended Kalman filter is applied to the system using nonlinear and Gaussian distributions to improve the tracking performance by reducing the measurement error.

Additional simulations were performed to show the consistency of the proposed system as shown in Figures 13 and 14. The results of Simulation 2 also show similar results to the previous results. Figure 14 shows an estimation error of about 20–30 m while the UAV tracks the flight target. Further, it shows that the estimation error decreases when the target stops moving. As a result, the simulation results ensured that the UAV succeeded in pursuing the target, but it was in an environment where various assumed conditions were satisfied. In a real environment, the error is larger, and the tracking performance may be reduced. We conducted field tests to verify and evaluate the proposed tracking strategy.

C. VALIDATION FOR THE TENDENCY OF RSSI

We analyzed the RSSI tendency according to the direction of the antenna and the relative distance of the target in a previous study [18]. To validate the proposed approach, an additional experiment was performed to identify the RSSI tendency according to the target direction. The distance between the antenna and target was set to maintain a constant distance of 50 m, and the heading angle of the antenna was set such that the dominant directional angle (0°) was toward the target. The target orientation was set to a total of eight cases at 45° intervals from 0° to 360°. The experimental results for RSSI tendencies are shown in Figure 15.

In the results of the statistical analysis for eight cases, the p-value was 0.770. Therefore, there was no significant difference between experimental cases. These results indicate that the target angle does not significantly affect the RSSI measurements when the antenna heading faces the tag. Nevertheless, in the case of 0°, 45°, and 315° of the target angle, the RSSI measurements showed better results on average than the other cases.

D. EXPERIMENTAL SETUP

As described in Sec. I-A, the technical problem to be solved in the case of flying insects is 2D-based localization and tracking, considering the sensor precision of radio tags. Therefore, we proved and evaluated the performance of the proposed approach using UGV instead of UAV for the preliminary tests.

First, we performed field tests in an outdoor environment using a sensor system and evaluated the localization performance under static conditions. Although this field test also substitutes flying insects with a static transmitter, a similar tendency can be obtained using the proposed system. However, signal interference with the transmitter may occur owing to uncertain environments when it is attached to a flying insect. Additionally, we used ground control software based on Google Maps to estimate and map the tracking robot and transmitter in this study. In the second experiment, a localization experiment was performed on a dynamic target experiment using a fixed receiver and a dynamic transmitter mounted on a ground mobile robot (Jackal).

Thirdly, we conducted experiments to evaluate the extended Kalman filter-based tracking strategy developed in this study by using two Jackal robots to implement a dynamic target and a dynamic tracking robot environment, as shown in Figure 16. In this experiment, the target Jackal was set to autonomously drive at 2 m/s to mimic the dynamic mobility of insects. In addition, a radio telemetry transmitter, whose tag could be attached to flying insects, was fixed to the target unmanned ground vehicle (UGV), which implemented a sensor system that could be attached to a tracking UAV. The

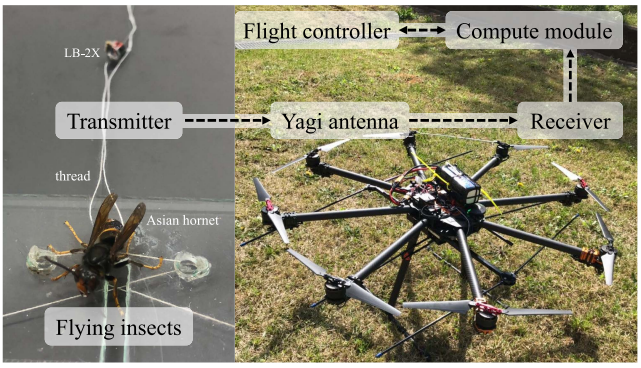

FIGURE 18. Autonomous tracking UAV system.

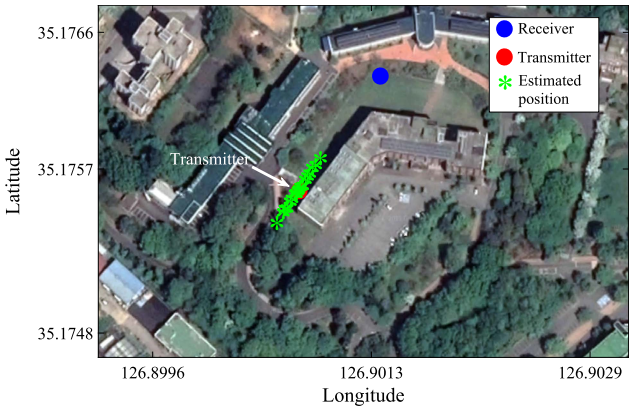

FIGURE 19. Experimental results of localization for a static target (scenario 1).

directional angle of the Yagi antenna (0°) was set to be the same as the heading angle of the static base and the mobile robot.

Finally, pixhawk-based octocopter was used for field tests to validate flight tracking system. Figure 18 shows the UAV system that we developed based on the design in Figure 6. A jig was also designed and affixed to the UAV to mount the tracking sensor system. For the field tests, we confirmed that the UAVs maintained stable hovering, regardless of the payload. To start the localization and tracking process, Wi-Fi communication was made with the ground control station and the UAV's onboard computer. The ground control station is set to observe the state of the UAV and to prepare for unexpected situations (e.g., collision accident) via UAV telemetry. In this study, we apply the experimental scenario in which the UAV estimates the position of a fixed radio-tagged flying target and tracks it autonomously. The case of a fixed flight target was considered because it was difficult to determine the ground truth for the position of the autonomous flight target.

E. RESULTS OF FIELD TESTS

For the feasibility test, the small-sized radio transmitter was fixed in a specific area to measure the reachable range of radio propagation. Considering the characteristics of the selected sensor system, it was confirmed that the ideal range was

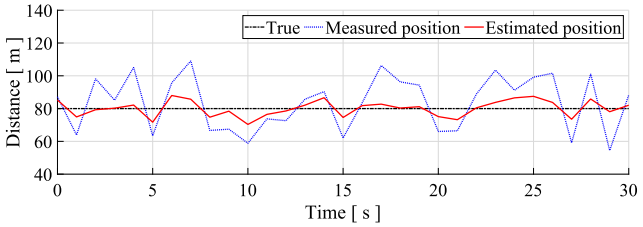

FIGURE 20. Estimation results of scenario 1.

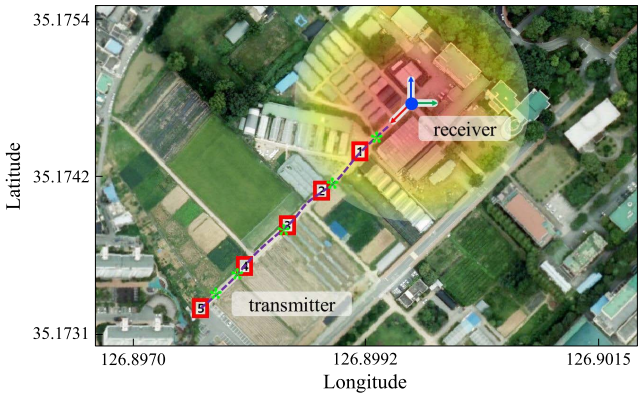

FIGURE 21. Experimental results of localization for a dynamic target (scenario 2).

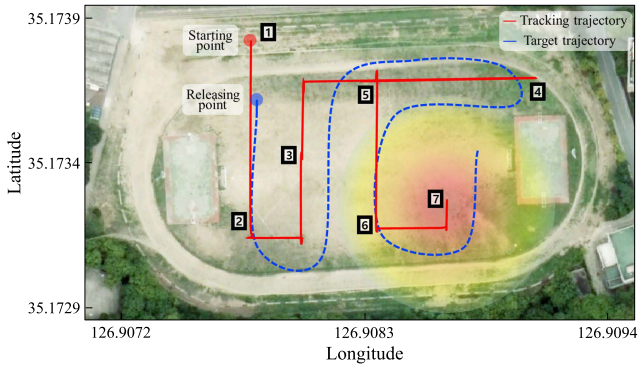

FIGURE 22. Results of feasibility tests for active tracking (scenario 3).

300—350 m (Figure 17), and the radio signal can be measured up to a distance of approximately 300 m in a real field [18]. The results of the first scenario for verifying localization using a fixed transmitter and receiver are shown in Figures. 19 and 20, respectively. The distance between the receiver and the target was 80 m, and the heading angles of the receiver and transmitter were set along a straight line. Here, the blue dot indicates a fixed receiver, the red dot indicates a fixed transmitter, and the green mark indicates the estimated position. Figure A shows the measured and estimated positions over time. The experimental results show that the root mean square error (RMSE) for the estimated position is 5.39 m and the standard deviation is 15.72 m. Because the transmitter is fixed and located in an open field, the error is relatively low.

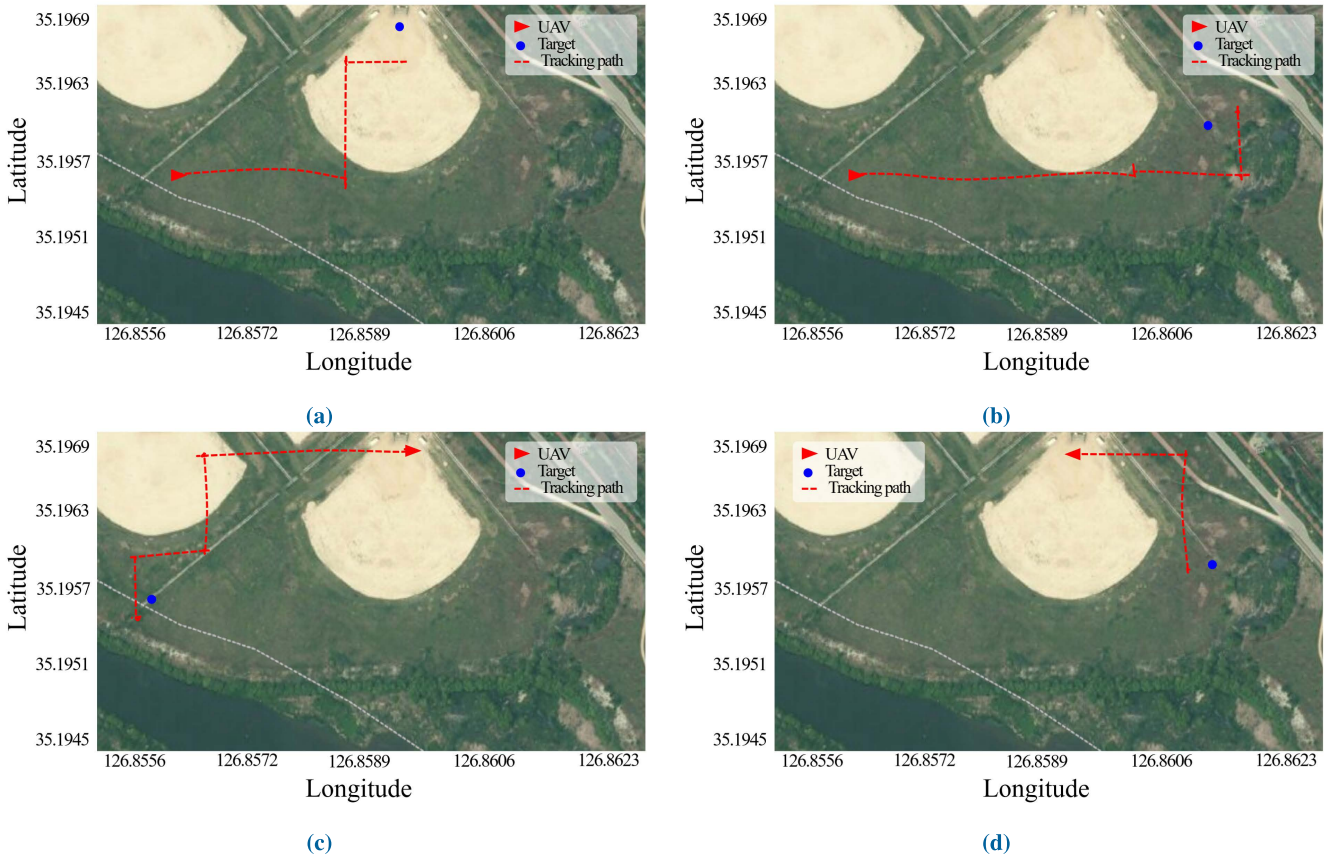

FIGURE 23. Experimental results of the UAV-based field test.

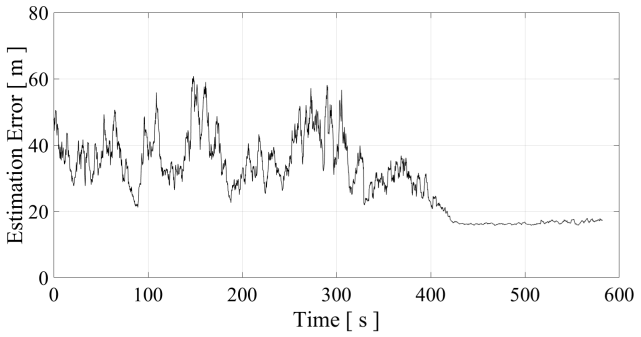

FIGURE 24. Experimental result of localization in case (c).

Figure 21 shows the results of a localization experiment for a stationary receiver and a dynamic transmitter (scenario 2). The experiment was performed by mounting the radio transmitter on Jackal UGV that was manually controlled by the operator without rotating the receiver. Here, the blue dot indicates the position of the receiver, the purple dotted line indicates the path of Jackal UGV, and the green mark represents the estimated location. The RMSEs for each specific time were 37.63 m for T_1, 15.29 m for T_2, 8.24 m for T_3, 12.80 m for T_4, and 33.19 m for T_5. If the relative distance between the receiver and transmitter is too low or too high, identifying the measured RSSI will be difficult because it includes noise that results in a large position error. Therefore, when the dynamic receiver is applied to the tracking system and maintains a proper distance, such as T_2, T_3, and T_4, it is possible to improve the localization accuracy of the dynamic target.

Figure 22 illustrates the experimental results obtained through field tests for the dynamic transmitter and active tracking system. The red line indicates the path of the tracking mobile robot, and the blue dotted line indicates the path of the radio-tagged mobile target. In the experimental results, the maximum RMSE between the estimated position and the actual position was found to be approximately 52.14 m (T_4). The mean of the RMSE is 31.04 m, and the standard deviation during the field tests is 12.37 m. Although the estimation results can be judged to be a significant error in actual tracking, these results are sufficient to track flying targets, and the tracking direction is relatively consistent, as shown in Figure 22. In this field test, the distance threshold was set to 25 m. When the experiment was completed, the actual relative distance was approximately 22.11 m, and the estimated relative distance through the localization algorithm was 20.83 m (T_7). The external noise reduces the localization performance in the case of dynamic flying targets or crowded fields. This field test sufficiently demonstrates the feasibility of the proposed approach and system.

In this feasibility study, the results were validated using a UGV instead of a UAV, but this should provide similar results. In (3), aerial tracking is possible by expanding the position of the target (x) and the observer ($\mathcal{O}$) in three dimensions. In addition, when using an aerial robot rather than a ground robot, the measurement accuracy of the RSSI is improved, which can yield better localization performance because the tracking robot can measure clear radio signals in the air [5].

Finally, Figures 23 and 24 represents the experimental results of the UAV-based field tests. These results show the flight path, starting position of the UAV, and target position. In this scenario, we apply the experimental case in which the UAV estimates the position of a fixed radio-tagged flying target and tracks it autonomously. The fixed flight target was only considered because it was difficult to determine the ground truth for the position of the autonomous flight target. Therefore, UAV with a constant altitude in the open field tracked the fixed target and completed the tracking process. Figure 24 shows the experimental results of localization for case (c) during the tracking process. These results represent a two-dimensional estimation error. There is an estimated error between 20 m and 60 m before 400 s. The estimation error at the end of the tracking process after 400 s converges to about 20 m. The experimental result, including uncertainty in localization, is the limitation of the sensor's hardware with a trade-off of weight and signal resolution. In these field tests, we designed experiments by changing the starting position of the UAV and the target position. Nevertheless, we confirmed successful cases in which a UAV-based tracking system tracked radio tags. The experimental results indicate that the relative distance between the UAV and the radio target was approximately 20 to 50 m after the tracking procedure.

Although we implemented an active tracking system based on the proposed strategy and evaluated its performance, there were limitations. In previous studies [5], [6], a UAV tracking system was developed for a large dynamic animal and tracked with a position error of approximately 20 to 40 m; however, this study used a small-sized transmitter with a weak RSS. Evidently, there are limits between the radio transmitter RSSI, reachable distance, and weight; however, the results presented in this study are sufficient for biologists and life scientists. Although the proposed approach is efficient for tracking radio-tagged flying insects, it should not be overlooked that most systems are nonlinear dynamic systems with complex disturbances in the natural environment. Therefore, if a particle filter or an unscented Kalman filter that further covers nonlinearity is applied in the developed system for more advanced tracking, the dynamic target can be estimated and tracked more efficiently [41]. Alternatively, an event-driven heterogeneous robot system (e.g., a radio-tracking UAV equipped with a thermal infrared camera [42]) is scalable and can be more useful than conventional systems for tracking radio-tagged flying targets [43].

F. DISCUSSIONS

In this study, we proposed a mobile robot-based tracking strategy for localizing and autonomously tracking radio-tagged flying insects. However, to track flying targets more accurately based on the developed system, the following are considered:

1) Turning time: it takes a significant amount of time for the mobile robot to rotate to measure the radio signal strength.
2) Tracking precision: the bearing angle is measured only in four directions.

To solve these problems, we consider the following directions for future research: (1) additional ground multiantenna systems and (2) gimbal-based rotary antenna systems.

An additional ground multiantenna system is a localization approach based on range-based measurements with an omnidirectional antenna. Because this method usually uses triangulation, it does not require the rotation of the Yagi antenna or UAV in the existing system. In addition, it is possible to more precisely optimize the existing range measurement based on the multisource of RSSI (i.e., high resolution of distance). Therefore, the presented research direction can address the problems of the turning time and the tracking precision.

The gimbal-based rotary antenna system is a localization approach that uses bearing-based measurements with a directional antenna. This method can replace the slow turning time of a UAV in an existing system with a fast gimbal rotation rate. In addition, the rotary antenna system can rotate optimally according to the sampling time (i.e., high angle resolution). Therefore, the presented bearing measurement method can improve the performance of the proposed system for a fast turning time and high tracking precision.

Furthermore, tracking strategies need to be improved to enhance the turning time and tracking precision. For example, if the UAV determines the target's flight direction through an initial 360° rotation, it may not be necessary to continue 360° turning during the tracking process. However, the bearing angle may be incorrectly estimated when the relative distance between the pursuer and the target is close. Therefore, this study proposes a tracking strategy based on 360° rotation to mitigate the environmental noise and improve the robustness of tracking. In future work, we plan to analyze the flight pattern of the Asian hornet and enhance the performance of the developed system, considering its practicality.

Moreover, in this study, the relative distance and bearing of the target were estimated through a range-only measurement. A bearing-only measurement is being studied as an alternative method [8], [44]. The bearing-only approach causes a long measurement time and a heavy payload [45]. However, a range-only approach leads to a relatively fast measurement time and light payload system [5], [46]. Therefore, in the case of this study, a range-only measurement method and a directional tracking strategy were selected in consideration of the limited performance of the radio telemetry system. However, a bearing-only measurement method may have to

be selected to deal with the estimation problem of getting too close to the flying target.

Nevertheless, the proposed system is relevant for tracking radio-tagged flying targets. To the best of our knowledge, no previous study has reported a mobile robot-based autonomous tracking system for a radio-tagged flying insects. The goal of this study is to track small targets while dealing with the limitations of the lightest sensor models among commercial radio tags. The tracking of flying insects such as Asian hornets is a practical problem in the real world. Humans directly tracked Asian hornets and destroyed the nests [32], and these actions can efficiently reduce the number of Asian wasps. Tracking flying insects remains a challenge, but our proposed system has sufficient feasibility.

In the case of practical tracking, the proposed system should take some problems into account. For example, noise generated by UAV could affect the behavior of flying insects. Because of limitations in sensor technologies, in our case, sensors with localization precision of tens of meters must be used to track flying insects. Therefore, the proposed concept is a mobile robot system acting as an observer and tracking in a distant location without being too close to an insect as described in Sec. I-A. As a result, we assume that this relative distance would not affect insect behavior in this study. Nevertheless, the effects of generated noise should be considered in future work.

In another example, radio sensors attached to flying insects can affect their flight capabilities, speed, and homing behavior. However, as shown in Tables 1 and 2, most studies have reported several successful cases, although they have sometimes failed to track tagged hornets. Although the success rate of tracking may vary depending on the biological characteristics of insects, this study proposes the traceability of flying insects with homing instinct and describes a UAV system to find their nests autonomously. As a result, this study focuses on the following questions: (1) how to localize the target from the radio signal strength, (2) how the mobile robot autonomously tracks the estimated position, and (3) how to design the system architecture for the implementation. Therefore, this study is valuable considering its traceable distance, robot-based mobility and autonomy, and the limitations of radio tags.

V. CONCLUSION

In this study, we proposed a mobile robot-based approach for tracking radio-tagged flying insects. Based on the filtered RSS, we proposed a strategy for UAVs to track flying insects autonomously and constructed/performed a dynamic simulation to validate the developed system. The simulation results demonstrate that the proposed method can estimate and track the position of the target. It was also confirmed that the UAV reached the final position of the habitat without losing the object. Although the position localization performance is not highly accurate, it can be improved sufficiently by integrating an advanced filter in a nonlinear system (e.g., a particle filter and an unscented Kalman filter). Furthermore, the feasibility and effectiveness of the proposed system were tested in the field. These experimental results validate the feasibility of the proposed approach. The system developed in this study can be used to track and manage small-sized animals and insects in the ecosystem. In future work, we plan to conduct practical experiments with flying insects.

REFERENCES

[1] J. I. Huircán, C. Muñoz, H. Young, L. Von Dossow, J. Bustos, G. Vivallo, and M. Toneatti, "ZigBee-based wireless sensor network localization for cattle monitoring in grazing fields," *Comput. Electron. Agricult.*, vol. 74, no. 2, pp. 258–264, 2010.

[2] R. Kays, S. Tilak, M. Crofoot, T. Fountain, D. Obando, A. Ortega, F. Kuemmeth, J. Mandel, G. Swenson, T. Lambert, B. Hirsch, and M. Wikelski, "Tracking animal location and activity with an automated radio telemetry system in a tropical rainforest," *Comput. J.*, vol. 54, no. 12, pp. 1931–1948, Nov. 2011.

[3] J. Kim, S. Kim, C. Ju, and H. I. Son, "Unmanned aerial vehicles in agriculture: A review of perspective of platform, control, and applications," *IEEE Access*, vol. 7, pp. 105100–105115, 2019.

[4] K. S. Christie, S. L. Gilbert, C. L. Brown, M. Hatfield, and L. Hanson, "Unmanned aircraft systems in wildlife research: Current and future applications of a transformative technology," *Frontiers Ecol. Environ.*, vol. 14, no. 5, pp. 241–251, 2016.

[5] H. V. Nguyen, M. Chesser, L. P. Koh, S. H. Rezatofighi, and D. C. Ranasinghe, "TrackerBots: Autonomous unmanned aerial vehicle for real-time localization and tracking of multiple radio-tagged animals," *J. Field Robot.*, vol. 36, no. 3, pp. 617–635, May 2019.

[6] O. M. Cliff, D. L. Saunders, and R. Fitch, "Robotic ecology: Tracking small dynamic animals with an autonomous aerial vehicle," *Sci. Robot.*, vol. 3, no. 23, p. eaat8409, Oct. 2018.

[7] F. Körner, R. Speck, A. H. Göktogan, and S. Sukkarieh, "Autonomous airborne wildlife tracking using radio signal strength," in *Proc. IEEE/RSJ Int. Conf. Intell. Robots Syst.*, Oct. 2010, pp. 107–112.

[8] O. M. Cliff, R. Fitch, S. Sukkarieh, D. L. Saunders, and R. Heinsohn, "Online localization of radio-tagged wildlife with an autonomous aerial robot system," in *Robotics: Science and Systems XI*, vol. 11, L. E. Kavraki, D. Hsu, and J. Buchli, Eds. Cambridge, MA, USA: MIT Press, Jul. 2015. [Online]. Available: http://www.roboticsproceedings.org/rss11/p42.html, doi: 10.15607/RSS.2015.XI.042.

[9] C. G. Müller, B. L. Chilvers, Z. Barker, K. P. Barnsdale, P. F. Battley, R. K. French, J. McCullough, and F. Samandari, "Aerial VHF tracking of wildlife using an unmanned aerial vehicle (UAV): Comparing efficiency of yellow-eyed penguin (*Megadyptes antipodes*) nest location methods," *Wildlife Res.*, vol. 46, no. 2, pp. 145–153, 2019.

[10] N. Hui, "Efficient drone-based radio tracking of wildlife," Ph.D. dissertation, Univ. California San Diego, La Jolla, CA, USA, 2019.

[11] M. Olivares-Mendez, C. Fu, P. Ludivig, T. Bissyandé, S. Kannan, M. Zurad, A. Annaiyan, H. Voos, and P. Campoy, "Towards an autonomous vision-based unmanned aerial system against wildlife poachers," *Sensors*, vol. 15, no. 12, pp. 31362–31391, Dec. 2015.

[12] P. Tokekar, D. Bhadauria, A. Studenski, and V. Isler, "A robotic system for monitoring carp in Minnesota lakes," *J. Field Robot.*, vol. 27, no. 6, pp. 779–789, Nov. 2010.

[13] M. A. Ditmer, J. B. Vincent, L. K. Werden, J. C. Tanner, T. G. Laske, P. A. Iaizzo, D. L. Garshelis, and J. R. Fieberg, "Bears show a physiological but limited behavioral response to unmanned aerial vehicles," *Current Biol.*, vol. 25, no. 17, pp. 2278–2283, Aug. 2015.

[14] F. Requier, Q. Rome, G. Chiron, D. Decante, S. Marion, M. Menard, F. Müller, C. Villemant, and M. Henry, "Predation of the invasive Asian hornet affects foraging activity and survival probability of honey bees in western Europe," *J. Pest Sci.*, vol. 92, no. 2, pp. 567–578, Mar. 2019.

[15] P. J. Kennedy, S. M. Ford, J. Poidatz, D. Thiéry, and J. L. Osborne, "Searching for nests of the invasive Asian hornet (*Vespa velutina*) using radio-telemetry," *Commun. Biol.*, vol. 1, no. 1, p. 88, Dec. 2018.

[16] R. Maggiora, M. Saccani, D. Milanesio, and M. Porporato, "An innovative harmonic radar to track flying insects: The case of *Vespa velutina*," *Sci. Rep.*, vol. 9, no. 1, pp. 1–10, Dec. 2019.

[17] C. J. Amlaner and D. W. Macdonald, "A handbook on biotelemetry and radio tracking," in *Proc. Int. Conf. Telemetry Radio Tracking Biol. Med.*, Oxford, U.K., 2013, pp. 20–22.

[18] S. Kim, C. Ju, J. Kim, and H. I. Son, "A tracking method for the invasive Asian hornet: A brief review and experiments," *IEEE Access*, vol. 7, pp. 176998–177008, 2019.
[19] B. Thomas, J. D. Holland, and E. O. Minot, "Wildlife tracking technology options and cost considerations," *Wildlife Res.*, vol. 38, no. 8, pp. 653–663, 2012.
[20] S. Särkkä, V. V. Viikari, M. Huusko, and K. Jaakkola, "Phase-based UHF RFID tracking with nonlinear Kalman filtering and smoothing," *IEEE Sensors J.*, vol. 12, no. 5, pp. 904–910, May 2012.
[21] G. A. M. D. Santos, Z. Barnes, E. Lo, B. Ritoper, L. Nishizaki, X. Tejeda, A. Ke, H. Lin, C. Schurgers, A. Lin, and R. Kastner, "Small unmanned aerial vehicle system for wildlife radio collar tracking," in *Proc. IEEE 11th Int. Conf. Mobile Ad Hoc Sensor Syst.*, Oct. 2014, pp. 761–766.
[22] A. M. Jensen, D. K. Geller, and Y. Chen, "Monte Carlo simulation analysis of tagged fish radio tracking performance by swarming unmanned aerial vehicles in fractional order potential fields," *J. Intell. Robot. Syst.*, vol. 74, no. 1, pp. 287–307, Apr. 2014.
[23] W. D. Kissling, D. E. Pattemore, and M. Hagen, "Challenges and prospects in the telemetry of insects," *Biol. Rev.*, vol. 89, no. 3, pp. 511–530, Aug. 2014.
[24] K. VonEhr, S. Hilaski, B. E. Dunne, and J. Ward, "Software defined radio for direction-finding in UAV wildlife tracking," in *Proc. IEEE Int. Conf. Electro Inf. Technol. (EIT)*, May 2016, pp. 0464–0469.
[25] Q. S. Le, J. Kim, J. Kim, and H. I. Son, "Report on work in progress of small insect tracking system using autonomous UAV," in *Proc. 14th Int. Conf. Ubiquitous Robots Ambient Intell. (URAI)*, Jun. 2017, pp. 242–243.
[26] M. Negro, E. Caprio, K. Leo, U. Maritano, A. Roggero, G. Vacchiano, C. Palestrini, and A. Rolando, "The effect of forest management on endangered insects assessed by radio-tracking: The case of the ground beetle *Carabus olympiae* in European beech *Fagus sylvatica* stands," *Forest Ecol. Manage.*, vol. 406, pp. 125–137, Dec. 2017.
[27] J. Poidatz, K. Monceau, O. Bonnard, and D. Thiéry, "Activity rhythm and action range of workers of the invasive hornet predator of honeybees *Vespa velutina*, measured by radio frequency identification tags," *Ecol. Evol.*, vol. 8, no. 15, pp. 7588–7598, Aug. 2018.
[28] X. F. Sánchez and R. J. Charles, "Notes on the nest architecture and colony composition in winter of the yellow-legged Asian hornet, *Vespa velutina* lepeletier 1836 (Hym.: Vespidae), in its introduced habitat in Galicia (NW Spain)," *Insects*, vol. 10, no. 8, p. 237, Aug. 2019.
[29] A. Perrard, J. Haxaire, A. Rortais, and C. Villemant, "Observations on the colony activity of the Asian hornet *Vespa velutina* Lepeletier 1836 (Hymenoptera: Vespidae: Vespinae) in France," *Annales Société Entomologique France*, vol. 45, no. 1, pp. 119–127, 2009.
[30] M. Leza, M. Á. Miranda, and V. Colomar, "First detection of *Vespa velutina nigrithorax* (hymenoptera: Vespidae) in the Balearic islands (Western Mediterranean): A challenging study case," *Biol. Invasions*, vol. 20, no. 7, pp. 1643–1649, Jul. 2018.
[31] J. Carvalho, D. Hipólito, F. Santarém, R. Martins, A. Gomes, P. Carmo, R. Rodrigues, J. Grosso-Silva, and C. Fonseca, "Patterns of *Vespa velutina* invasion in Portugal using crowdsourced data," *Insect Conservation Diversity*, vol. 13, no. 5, pp. 501–507, Sep. 2020.
[32] M. Leza, C. Herrera, G. Picó, T. Morro, and V. Colomar, "Six years of controlling the invasive species *Vespa velutina* in a Mediterranean island: The promising results of an eradication plan," *Pest Manage. Sci.*, vol. 77, no. 5, pp. 2375–2384, May 2021.
[33] S. G. Compton, M. D. Ellwood, A. J. Davis, and K. Welch, "The flight heights of chalcid wasps (hymenoptera, chalcidoidea) in a lowland Bornean rain forest: Fig wasps are the high fliers[1]," *Biotropica*, vol. 32, no. 3, pp. 515–522, 2000.
[34] R. D. Harrison, "Fig wasp dispersal and the stability of a keystone plant resource in Borneo," *Proc. Roy. Soc. London B, Biol. Sci.*, vol. 270, no. 1, pp. S76–S79, Sep. 2003.
[35] S. G. Compton, M. Ellwood, R. Low, and J. Watson, "Dispersal of fig wasps (Hymenoptera: Chalcidoidea) across primary and logged rainforest in Sabah (Malaysia)," *Acta Soc. Zoologicae Bohemicae*, vol. 69, pp. 1–12, Jan. 2005.
[36] N. Jeevanandam and R. Corlett, "Fig wasp dispersal in urban Singapore," *Raffles Bull. Zool.*, vol. 61, pp. 343–347, Feb. 2013.
[37] D. Sauvard, V. Imbault, and É. Darrouzet, "Flight capacities of yellow-legged hornet (*Vespa velutina nigrithorax*, hymenoptera: Vespidae) workers from an invasive population in Europe," *PLoS ONE*, vol. 13, no. 6, Jun. 2018, Art. no. e0198597.
[38] L. Dressel and M. J. Kochenderfer, "Hunting drones with other drones: Tracking a moving radio target," in *Proc. Int. Conf. Robot. Automat. (ICRA)*, May 2019, pp. 1905–1912.
[39] S. J. Julier and J. K. Uhlmann, "New extension of the Kalman filter to nonlinear systems," *Proc. SPIE*, vol. 3068, pp. 182–193, Apr. 1997.
[40] J. B. Andersen, T. S. Rappaport, and S. Yoshida, "Propagation measurements and models for wireless communications channels," *IEEE Commun. Mag.*, vol. 33, no. 1, pp. 42–49, Jan. 1995.
[41] I. Ullah, X. Su, J. Zhu, X. Zhang, D. Choi, and Z. Hou, "Evaluation of localization by extended Kalman filter, unscented Kalman filter, and particle filter-based techniques," *Wireless Commun. Mobile Comput.*, vol. 2020, pp. 1–15, Oct. 2020.
[42] S. Lioy, E. Bianchi, A. Biglia, M. Bessone, D. Laurino, and M. Porporato, "Viability of thermal imaging in detecting nests of the invasive hornet *Vespa velutina*," *Insect Sci.*, vol. 28, no. 1, pp. 271–277, Feb. 2021, doi: 10.1111/1744-7917.12760.
[43] C. Ju and H. I. Son, "Modeling and control of heterogeneous agricultural field robots based on Ramadge–Wonham theory," *IEEE Robot. Autom. Lett.*, vol. 5, no. 1, pp. 48–55, Jan. 2020.
[44] J. V. Hook, P. Tokekar, and V. Isler, "Cautious greedy strategy for bearing-only active localization: Analysis and field experiments," *J. Field Robot.*, vol. 31, no. 2, pp. 296–318, Mar. 2014.
[45] H. Bayram, N. Stefas, K. S. Engin, and V. Isler, "Tracking wildlife with multiple UAVs: System design, safety and field experiments," in *Proc. Int. Symp. Multi-Robot Multi-Agent Syst. (MRS)*, Dec. 2017, pp. 97–103.
[46] H. V. Nguyen, F. Chen, J. Chesser, H. Rezatofighi, and D. Ranasinghe, "LAVAPilot: Lightweight UAV trajectory planner with situational awareness for embedded autonomy to track and locate radio-tags," in *Proc. IEEE/RSJ Int. Conf. Intell. Robots Syst. (IROS)*, Oct. 2020, pp. 2488–2495.

CHANYOUNG JU (Student Member, IEEE) received the B.S. and M.S. degrees from the Department of Rural and Biosystems Engineering, Chonnam National University, South Korea, in 2017 and 2019, respectively, where he is currently pursuing the Ph.D. degree in biosystems engineering. His research interests include field robotics, supervisory control, discrete event systems, and hybrid systems.

HYOUNG IL SON (Senior Member, IEEE) received the B.S. and M.S. degrees from the Department of Mechanical Engineering, Pusan National University, South Korea, in 1998 and 2000, respectively, and the Ph.D. degree from the Department of Mechanical Engineering, Korea Advanced Institute of Science and Technology (KAIST), South Korea, in 2010. He also had several appointments both academia and industry as a Senior Researcher with LG Electronics, Pyeongtaek-si, South Korea, from 2003 to 2005, and Samsung Electronics, Cheonan, South Korea, from 2005 to 2009; a Research Associate with the Institute of Industrial Science, The University of Tokyo, Tokyo, Japan, in 2010; and a Research Scientist with the Max Planck Institute for Biological Cybernetics, Tübingen, Germany, from 2010 to 2012. From 2012 to 2015, he leads the Telerobotics Group, Central Research Institute, Samsung Heavy Industries, Daejeon, South Korea, as a Principal Researcher. He joined the Faculty of the Department of Rural and Biosystems Engineering, Chonnam National University, Gwangju, South Korea, in 2015, where he is currently an Associate Professor. His research interests include field robotics, agricultural robotics, haptics, teleoperation, and discrete event and hybrid systems.